







Enhanced reactive oxygen detoxification occurs in salt-stressed soybean roots expressing *GmSALT3*

Yue Qu¹  | Rongxia Guan²  | Lili Yu² | Oliver Berkowitz³  | Rakesh David¹ | James Whelan³  | Melanie Ford¹ | Stefanie Wege¹  | Lijuan Qiu² | Matthew Gilliham¹ 

¹ARC Centre of Excellence in Plant Energy Biology, Waite Research Institute & School of Agriculture, Food and Wine, University of Adelaide, Glen Osmond, South Australia, Australia

²The National Key Facility for Crop Gene Resources and Genetic Improvement, Institute of Crop Science, Chinese Academy of Agricultural Sciences, Beijing, China

³Department of Animal, Plant and Soil Science, School of Life Science, Australian Research Council Centre of Excellence in Plant Energy Biology, La Trobe University, Bundoora, Victoria, Australia

Correspondence

Matthew Gilliham and Stephanie Wege, ARC Centre of Excellence in Plant Energy Biology, Waite Research Institute & School of Agriculture, Food and Wine, University of Adelaide, Glen Osmond, SA, Australia.
Email: matthew.gilliham@adelaide.edu.au and stefanie.wege@adelaide.edu.au

Lijuan Qiu, The National Key Facility for Crop Gene Resources and Genetic Improvement, Institute of Crop Science, Chinese Academy of Agricultural Sciences, Beijing, China.
Email: qiu lijuan@caas.cn

Funding information

Centre of Excellence in Plant Energy Biology, Australian Research Council, Grant/Award Number: CE140100008; Australian Research Council, Grant/Award Numbers: DE160100804, FT130100709; Chinese Academy of Agricultural Sciences; Natural Science Foundation of China, Grant/Award Number: 31830066

Edited by: J. Flexas

Abstract

Soybean (*Glycine max*) is an important crop globally for food and edible oil production. Soybean plants are sensitive to salinity (NaCl), with significant yield decreases reported under saline conditions. *GmSALT3* is the dominant gene underlying a major QTL for salt tolerance in soybean. *GmSALT3* encodes a transmembrane protein belonging to the plant cation/proton exchanger (CHX) family, and is predominately expressed in root phloem and xylem associated cells under both saline and non-saline conditions. It is currently unknown through which molecular mechanism(s) the ER-localised *GmSALT3* contributes to salinity tolerance, as its localisation excludes direct involvement in ion exclusion. In order to gain insights into potential molecular mechanism(s), we used RNA-seq analysis of roots from two soybean NILs (near isogenic lines); NIL-S (salt-sensitive, *Gmsalt3*), and NIL-T (salt-tolerant, *GmSALT3*), grown under control and saline conditions (200 mM NaCl) at three time points (0 h, 6 h, and 3 days). Gene ontology (GO) analysis showed that NIL-T has greater responses aligned to oxidation reduction. ROS were less abundant and scavenging enzyme activity was greater in NIL-T, consistent with the RNA-seq data. Further analysis indicated that genes related to calcium signalling, vesicle trafficking and Casparian strip (CS) development were upregulated in NIL-T following salt treatment. We propose that *GmSALT3* improves the ability of NIL-T to cope with saline stress through preventing ROS overaccumulation in roots, and potentially modulating Ca²⁺ signalling, vesicle trafficking and formation of diffusion barriers.

Yue Qu, Rongxia Guan, and Lili Yu contributed equally to this work.

This is an open access article under the terms of the [Creative Commons Attribution-NonCommercial](https://creativecommons.org/licenses/by-nc/4.0/) License, which permits use, distribution and reproduction in any medium, provided the original work is properly cited and is not used for commercial purposes.

© 2022 The Authors. *Physiologia Plantarum* published by John Wiley & Sons Ltd on behalf of Scandinavian Plant Physiology Society.

1 | INTRODUCTION

Plants use reactive oxygen species (ROS) as signalling molecules at low concentrations to regulate various biological processes, such as growth, programmed cell death, hormone signalling and development (Foreman et al., 2003; Mittler, 2002; Neill et al., 2002; Overmyer et al., 2003; Pei et al., 2000). However, ROS are also a toxic by-product of many reactions, which subsequently need to be eliminated by ROS scavenging enzymes. Under non-stressed conditions the production of ROS and the capacity of the cell to scavenge them are generally at equilibrium (Foyer & Noctor, 2005). However, under biotic and abiotic stresses, such as salinity, drought, temperature extremes, flooding, heavy metals, nutrient deprivation, and pathogen attack, intracellular ROS levels can increase dramatically. ROS at high concentrations damage plant cells through lipid peroxidation, DNA damage, protein denaturation, carbohydrate oxidation, and enzymatic activity impairment leading to significant damage to cellular functions and even cell death (Foyer & Noctor, 2005; Gill & Tuteja, 2010; Mittler et al., 2004; Noctor & Foyer, 1998). ROS damage due to environmental stress is therefore a leading factor contributing to reduced global crop production. ROS have, for example, detrimental effects on membrane integrity under drought stress and cause early senescence, lowering crop yield (Mittler, 2002; Sharma et al., 2017). In plants, ROS are eliminated through enzymatic and non-enzymatic pathways. Enzymatic antioxidant systems include scavenger enzymes such as SOD (superoxide dismutase), APX (ascorbate peroxidase), GPX (glutathione peroxidases), PrxR (proxiredoxin), GST (glutathione-S-transferase), and CAT (catalase); while non-enzymatic pathways include low molecular metabolites, such as ASH (ascorbate), GSH (glutathione), proline, α -tocopherol (vitamin E), carotenoids and flavonoids (Choudhury et al., 2017; Mittler et al., 2004).

Among the above-mentioned stresses, salinity is one of the most prominent factors restricting crop production and agricultural economic growth worldwide. More than US\$12 billion in revenue is estimated to be lost annually because of saline-affected agricultural land areas (Bose et al., 2014; Flowers et al., 2010; Gilliham et al., 2017). Soybean (*Glycine max* [L.] Merrill) is an important legume crop that contributes 30% of the total vegetable oil consumed and 69% of human food and animal feed protein-rich supplements (Lam et al., 2010; Prakash et al., 2001). The yield of soybean can be significantly reduced by salinity stress, especially during the early vegetative growth stage (Pi et al., 2016).

In soybean, *GmSALT3* (also known as *GmCHX1* and *GmNcl*) has been identified as a dominant gene that confers improved salinity tolerance (Do et al., 2016; Guan et al., 2014; Qi et al., 2014). It is mainly expressed in root phloem- and xylem-associated cells and the protein is localised in the ER (endoplasmic reticulum), not the plasma membrane (PM) (Guan et al., 2014). NILs (near isogenic lines), differing through a naturally occurring transposon insertion in the *GmSALT3* gene, have been used to show that *GmSALT3* is involved in shoot exclusion of both Na^+ (sodium) and Cl^- (chloride). In NILs with a functional *GmSALT3*, leaf Cl^- exclusion can be observed prior to Na^+ exclusion (Liu et al., 2016), suggesting two distinct mechanisms for

the exclusion of the two ions. Reciprocal grafting of NILs showed that shoot Na^+ exclusion occurs via a root xylem-based mechanism and shoot Cl^- exclusion likely depends upon novel phloem-based Cl^- recirculation (Qu et al., 2021). Additionally, *GmSALT3* is also related to K^+ homeostasis (Do et al., 2016; Qu et al., 2021). Despite the known importance of *GmSALT3* for soybean salinity tolerance, the molecular mechanism through which the ER-localised *GmSALT3* contributes to improved salinity stress tolerance has not yet been revealed.

High-throughput “-omics” technologies, including transcriptomics, proteomics, and metabolomics have been applied in an attempt to understand soybean root responses to salinity stress (Aghaei et al., 2009; Ge et al., 2010; Lu et al., 2013; Pi et al., 2016; Qin et al., 2013; Toorchi et al., 2009). While these studies provide a basis for examining the general responses of soybean roots to salt stress, they compare genetically diverse soybeans that differ in many aspects. For instance, proteomic studies utilising the cultivar Wenfeng07 (relatively salt-tolerant) and Union85140 (relatively salt-sensitive), suggested that Wenfeng07's tolerance to salinity stress was associated with flavonoid accumulation. Wenfeng07 contains the *GmSALT3* salt tolerant allele and it is absent in Union85140, and flavonoids belong to the metabolites that scavenge ROS. Several key enzymes in flavonoid synthesis including chalcone synthase (CHS), chalcone isomerase (CHI) and cytochrome P450 monooxygenase (CPM) were differently expressed in Wenfeng07 (Pi et al., 2016), suggesting a possible link between ROS detoxification and salinity tolerance in these two diverse soybean cultivars. However, less genetically diverse material is needed to demonstrate an explicit and direct link between ROS detoxification and *GmSALT3*.

We took advantage of our previously isolated NILs, and performed RNA-sequencing of NIL-T (salt-tolerant, *GmSALT3*) and NIL-S (salt-sensitive, *Gmsalt3*) roots, to further investigate the mechanism by which *GmSALT3* confers salinity tolerance. Genes connected to ROS signalling were significantly differently regulated in NIL-T compared to NIL-S under saline conditions, suggesting a direct connection of ROS production to *GmSALT3*. Enzymatic assays further revealed that presence of *GmSALT3* is essential for maintaining ROS homeostasis under saline conditions. Differential gene expression under control conditions suggested that NIL-S might be primed for responding to biotic stress in comparison to NIL-T.

2 | MATERIALS AND METHODS

2.1 | Plant growth conditions and stress treatments

NIL-T (salt-tolerant, *GmSALT3*) and NIL-S (salt-sensitive, *Gmsalt3*) plants were grown in a growth chamber (RXZ-500D; Ningbo Jiangnan Instrument), with a day length of 16 h (with a light-emitting diode light source at $400 \mu\text{mol m}^{-2} \text{s}^{-1}$) at 28°C , and 8 h dark at 25°C , with 60% relative humidity throughout. Soybean seedlings were treated with 200 mM NaCl (salt treatment) or water (control) at 10 days after sowing (DAS). 200 mM NaCl or water were applied again at 12 DAS.

2.2 | Total RNA extraction and RNA-seq library construction

Total RNA was extracted from soybean roots using TRIZOL reagent (Ambion, <http://www.ambion.com>). Whole roots were harvested at three time points, 0 h, 6 h, and 3 days of a 200 mM salt-treatment with the corresponding non-treatment controls. All the harvested soybean roots did not have nitrogen-fixing nodules and were not inoculated with symbiotic nitrogen fixing bacteria. To remove the residual DNA, the extracted RNA was treated with RNase-free DNase I (New England Biolabs, <https://www.neb.com>) for 30 min at 37°C. Thirty RNA libraries were generated for paired-end reads using an Illumina HiSeq 2500 sequencer, consisting of three biological samples per time point per genotype.

2.3 | RNA-seq data analysis and assembly

Raw reads were generated and mapped to the latest soybean genome sequence Gmax_275 Wm82.a2.v1 (Glyma 2.0) using TopHat2 (Kim et al., 2013). Clean mapped reads were obtained by removing low quality ($Q < 30$) sequences, adapter fragments and barcode sequences. A quality control test by fastQC (Andrews, 2010) revealed the quality of RNA-seq libraries construction and sequence alignment were sufficient for further analysis.

2.4 | Gene expression level and DEG analysis

Gene expression was compared in FPKMs (Fragments Per Kilobase of transcript per Million) calculated using the Cufflinks functions cuffquant and cuffnorm (Trapnell et al., 2012). Differential expression analysis of two conditions/groups was performed using the DESeq R package (1.10.1). The resulting p -values were adjusted using the Benjamini and Hochberg's approach for controlling the false discovery rate. The cutoffs for differentially expressed genes (DEGs) were Log_2FC (fold change) ≥ 1 , FDR (false discover rate) < 0.01 .

2.5 | GO enrichment and KEGG pathway analysis

GO enrichment analysis of DEGs was implemented using AgriGO (Du et al., 2010). GO terms with corrected p values < 0.05 were deemed significantly enriched. KEGG (Kanehisa et al., 2007) is a database resource for understanding high-level functions and utilities of the biological system, such as the cell, the organism and the ecosystem, from molecular-level information, especially large-scale molecular datasets generated by genome sequencing and other high-throughput experimental technologies (<http://www.genome.jp/kegg/>). We used KOBAS (Mao et al., 2005) software to test the statistical enrichment of differential expression genes in KEGG pathways.

2.6 | Weighted gene co-expression network analysis (WGCNA)

There were 54,175 genes annotated in all the RNA-seq libraries. After filtering out non-expressed genes, low-expressed genes (FPKM < 2) and genes that possessed large expression variation across replicates, 28,223 genes were selected for WGCNA analysis. An unsigned gene co-expression network was built using the WGCNA R-package (Langfelder & Horvath, 2008). The topological overlap measure (TOM) was calculated using the adjacency matrix between all genes with a power of 18. A gene dendrogram was created by using the dissimilarity TOM. Branches of the dendrogram (Figure S6) indicated modules (clustered highly co-expressed genes) through using the dynamic tree cut algorithm (Langfelder et al., 2008). Each module has an assigned colour. Similar modules were merged by calculating module eigengenes. Using the module eigengenes, the module-trait relationships (MTRs) were plotted by calculating the Pearson's correlations between the module eigengene and the samples (traits). A correlation of 0.75 with at least one of the selected traits was the criteria used to generate modules. Clustered genes in modules of interest were then used for further analysis. Genes annotation and GO term analysis were performed in Soybase (Grant et al., 2010) and AgriGO (Du et al., 2010), respectively.

2.7 | ROS production and contents measurement

Fourteen-day-old NIL-T and NIL-S soybean seedlings were used to measure the generation of ROS in roots. Roots were labelled with 30 μM dichlorofluorescein diacetate (DCFDA; Sigma-Aldrich), by incubating washed soybean roots for 10 min at room temperature in the dark with 30 μM DCFDA. ROS sensitive fluorescent dyes were imaged using a Nikon SMZ25 stereo microscope (Nikon). The excitation and emission wavelengths were 488 nm and 500/535 nm, respectively. Fluorescence intensity was measured by ImageJ/FIJI (Schindelin et al., 2012), signal intensity values were normalised by setting the mean value for NIL-T control to 1. Superoxide (O_2^-) anions were also measured followed by Li et al. (2019), using 0.2% NBT (nitroblue tetrazolium) in 50 mM sodium phosphate buffer (pH 7.5). Soybean root samples were submerged in NBT staining solution for 10 min, which was the time it took samples to develop the dark blue colour.

ROS contents in soybean root samples were measured using Amplex[®] UltraRed reagent (Invitrogen, USA). Sodium phosphate buffer (0.5 ml 50 mM pH 7.4) was added to 0.1 g soybean powder, after mixing and solubilisation, samples were set on ice for 5 min. Then tubes were centrifuged at 12,000g for 20 min. 500 μl supernatant was transferred into new tubes. An equal volume of 2:1 (vol/vol) chloroform:methanol was added and centrifuged at 12,000g for 5 min. 50 μl aqueous phase was taken from each sample and added into each well of 96-well microplate. 50 μl working solution (freshly made) was added into each well. Plates were incubated at 25°C for 30 min (protected from light). Fluorescence was measured at 540/590 nm.

2.8 | Scavenging activity of the superoxide anion (O_2^-) assay

The scavenging activity assay was adapted from Pi et al. (2016) with slight modifications. Less root homogenate (0.1 g) was used for measurement. Antioxidant enzymes were extracted with 2 ml of 0.05 M phosphate buffer (pH 5.5) from 0.1 g root homogenate. The extract was then centrifuged at 12,000g (4°C) for 10 min. Supernatant (40 μ l) was added into 160 μ l reaction buffer, which contained 80 μ l phosphate buffer, 40 μ l 0.05 M guaiacol (Sigma, USA), 40 μ l 2% hydrogen peroxide (H_2O_2). The increased absorbance at 470 nm in 96-well plates due to the enzyme-dependent guaiacol oxidation was recorded every 30 s until 4 min of reaction.

2.9 | Real-time quantitative reverse-transcription polymerase chain reaction (RT-qPCR) validation for RNA-seq results

Total RNA was extracted from soybean root tissues using the TRIZOL reagent (Ambion, <http://www.ambion.com>). To remove residual DNA, the extracted RNA was treated with RNase-free DNase I (New England Biolabs, <https://www.neb.com>) for 30 min at 37°C. For gene expression, first-strand cDNA synthesis was performed with a PrimeScript RT Reagent Kit (TaKaRa, <http://www.takara.co.jp/english>). Real-time PCR was performed using SYBR Premix Ex Taq II (TiRNaseH Plus) (TaKaRa). The level of *GmSALT3* transcript was normalised using the control gene *GmUKN1* (Hu et al., 2009).

3 | RESULTS

3.1 | RNA-sequencing preparation and profiles

GmSALT3 has previously been shown to be expressed in roots, and grafting experiments have shown that presence of *GmSALT3* expression in roots is sufficient to confer shoot Na^+ and Cl^- exclusion (Guan et al., 2014; Qu et al., 2021). Total root RNA was extracted from NIL-T and NIL-S, and transcriptomes obtained using RNA-seq in a time course from plants grown under control and saline conditions. To investigate short- and long-term responses, root samples were harvested at three time points, 0 h (control), 6 h, and 3 days with 200 mM salt-treatment and controls (Figure 1A and B) and in biological triplicates. Thirty RNA libraries were generated for paired-end reads using an Illumina HiSeq 1500 sequencer. In total, 1.6 billion paired 100bp raw reads were generated and mapped to the soybean genome sequence Gmax_275 Wm82.a2.v1 (Glyma 2.0) using TopHat2 (Kim et al., 2013). The average mapping percentage was 81.25%. After trimming of low quality ($Q < 30$), adapter fragments and barcode sequences, a total of 804 million clean mapped reads were identified. Combined with a quality control test using fastQC (Andrews, 2010), the quality of RNA-seq libraries construction and sequence alignment

was deemed sufficient for further analysis. A summary of mapped reads and quality of sequencing is shown in Table S1. Transcripts corresponding to *GmSALT3/Gmsalt3* in the NIL-T and NIL-S in all samples were confirmed. NIL-T transcriptomes contained reads across the entire full-length transcript for *GmSALT3* were obtained, while in NIL-S reads only mapped to the predicted truncated version *Gmsalt3* (Figure 1C). The phenotype of plants grown at the same time but not harvested and retained in the salt treatment after 10 days are shown in Figure 1D, to show the differential downstream impact of salt on NIL-T and NIL-S. A flowchart of data analysis is shown in Figure 1E.

3.2 | Overview of DEGs between NIL-T and NIL-S under control conditions

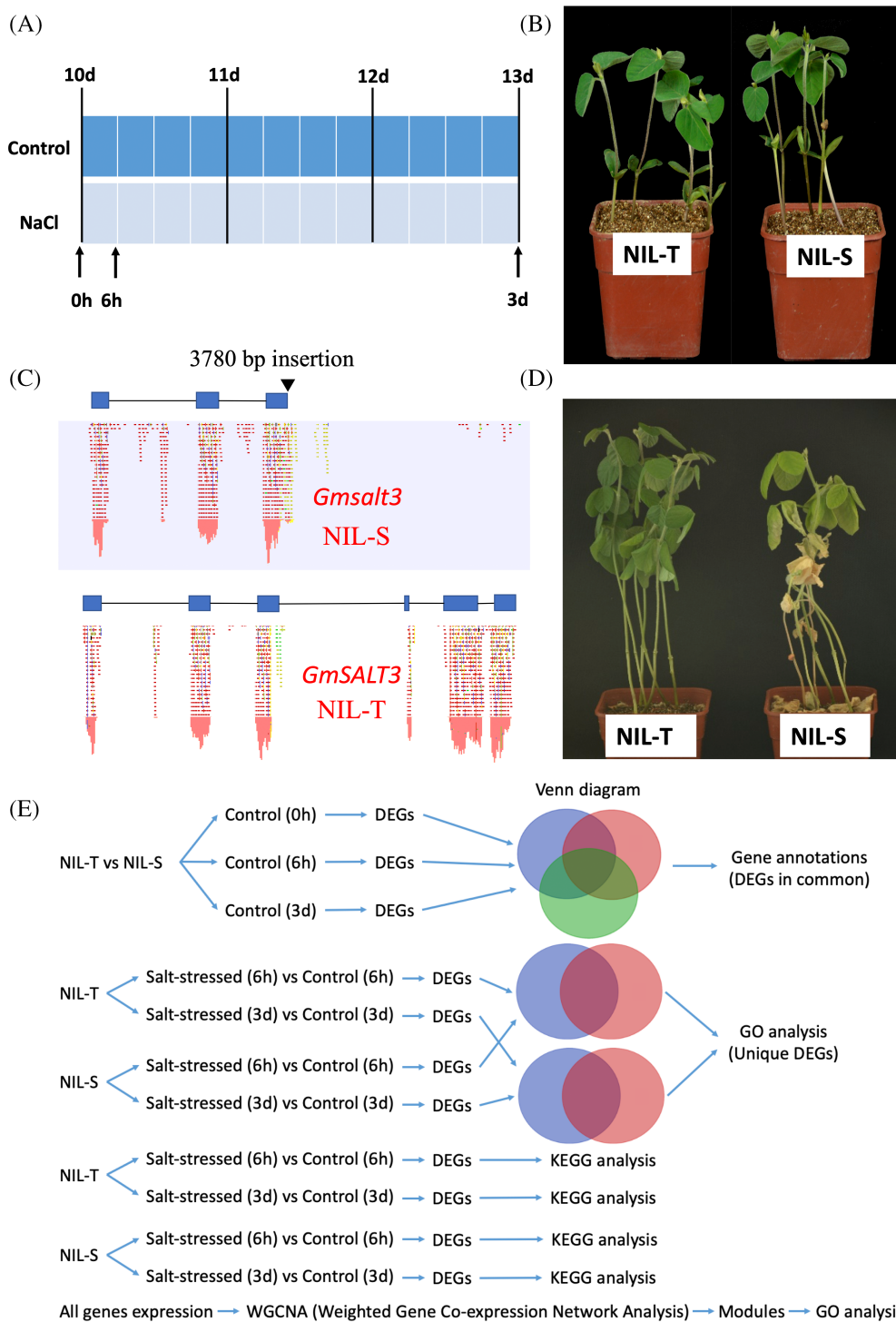
Previous work had shown that *GmSALT3* is expressed under both control and saline conditions, suggesting that there might already be a difference in other gene expression between NIL-T and NIL-S under control conditions. We therefore first compared the transcriptomes of NIL-T and NIL-S (indicated as “T” and “S”, respectively) under control conditions, before analysing changes due to salinity treatment. A PCA plot (for the first two principal components) of 10 grouped samples shows a good separation between all comparisons, confirming replicates clustered together consistently. Those comparisons are: Control 0 h T versus Control 0 h S (grey), Control 3 days T versus Control 3 days S (purple), and Control 6 h T versus Control 6 h S (brown) (Figure 2A). Transcript abundance was compared in FPKMs calculated using the Cufflinks functions cuffquant and cuffnorm (Trapnell et al., 2012). DEGs were classified as genes with a Log_2FC (fold change) ≥ 1 and a FDR (false discover rate) < 0.01 when comparing between two conditions.

There are 5 upregulated differentially expressed genes (DEGs) at 0 h, 9 upregulated DEGs at 6 h, and 6 upregulated DEGs at 3 days in NIL-S (compared to NIL-T), and a Venn diagram demonstrates 3 of these genes are common across three time points. There were 1, 5, and 5 downregulated DEGs at 0 h, 6 h, and 3 days, respectively, but the identity of the downregulated DEGs were different between each of the time point (Figure 2B). The three consistently upregulated DEGs in NIL-S at all time points under control conditions were *Glyma.07G196800* (Linoleate 13S-lipoxygenase 3-1), *Glyma.10G143600* (uncharacterized protein), and *Glyma.20G105500* (3-hydroxybenzoate 6-hydroxylase 1-like) (Figure 2C). Figure 2D shows the expression profile (in FPKM, fragments per kilobase of transcript per million) of these three genes at all time points of NIL-T and NIL-S under control conditions.

3.3 | Overview of DEGs in salt treated NIL-T and NIL-S when compared to their respective controls

Gene expression differences in response to salt of each genotype was then examined. By comparing control to salt treated NIL-T, we

FIGURE 1 Treatment, sampling strategy and data analysis. (A) Soybean seedlings were treated with 200 mM NaCl (salt treatment) or water (control) at 10 days after sowing (DAS). Arrows mean the sampling time points (0 h, 6 h, 3 days), triangle indicated the time point when water or NaCl solution was applied. (B) Pictures of soybean that had been treated with NaCl solution for 3 days. (C) Mapped reads to *GmSALT3* (bottom) and *Gmsalt3* (above). (D) The phenotype of NIL-T and NIL-S after 11 days salt treatment. (E) Flowchart of data analysis. NIL-T, NIL with *GmSALT3* allele; NIL-S, NIL with *Gmsalt3* allele; DEGs, differentially expressed genes; GO, gene ontology



identified 1816 DEGs that were differently expressed in NIL-T roots in response to salt (1263 upregulated and 553 downregulated, 6 h T). We then compared expression of control and salt treated NIL-S, and after 6 h salt treatment NIL-S roots (when compared to control NIL-S) showed a greater initial response in term of DEGs than we found in NIL-T, with a total of 3054 DEGs (1911 upregulated and 1143 downregulated, 6 h S) (Figure 3B). After 3 days of salt treatment, the increased number of DEGs in NIL-S was not observed anymore. On

the contrary, the NIL-T now showed a slightly higher number of DEGs compared to control conditions. NIL-T had 2844 DEGs (1333 upregulated and 1511 downregulated, 3 days T) while there were 2573 DEGs (1318 upregulated and 1255 downregulated, 3 days S) in NIL-S roots (Figure 3B).

Hierarchical clustering of the DEGs of the three replicates in different grouped samples is shown in Figure 3C-F. These DEGs represent the genes in each soybean NIL that are up- or downregulated in

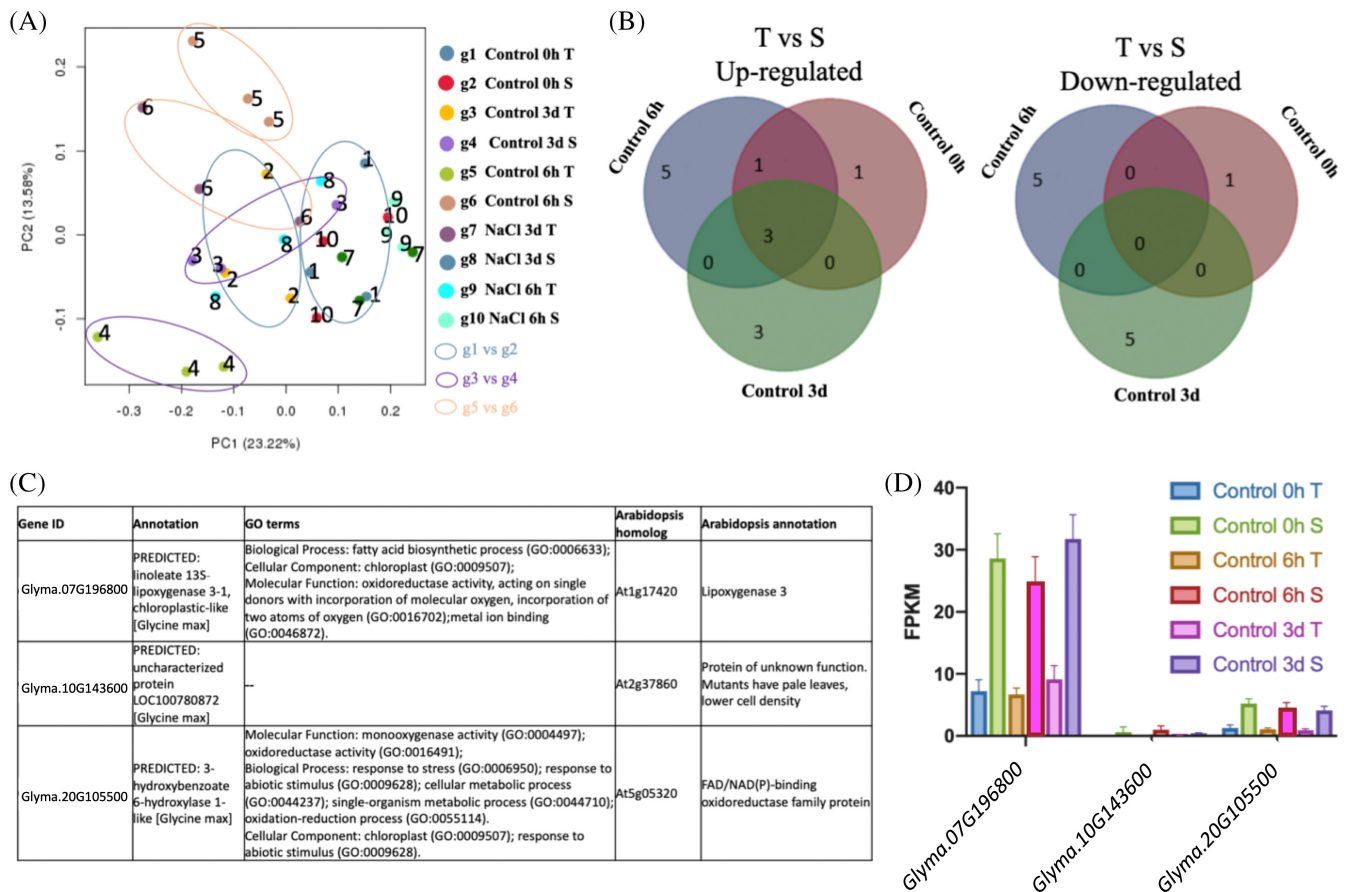


FIGURE 2 Overview of DEGs between NIL-T salt-tolerant and NIL-S salt-sensitive soybean samples at the 0 h, 6 h, and 3 days timepoints under non-saline conditions. (A) PCA plot of 10 groups (g1 – g10). Different coloured dots represent replicates in each group, different coloured circles represent comparisons between groups (g1 vs. g2, g3 vs. g4, g5 vs. g6). (B) Venn diagram of up- and downregulated DEGs in NIL-S soybeans at 0 h, 6 h, and 3 days under control conditions. (C) Three up-regulated DEGs in NIL-S soybeans at all 0 h, 6 h, and 3 days under control conditions, and their expression profile is shown in (D). The cutoffs for DEGs are Log_2FC (fold change) ≥ 1 , FDR (false discover rate) < 0.01 .

response to salt. We used the hierarchical clustering to identify DEGs, which either similarly change in expression in the two genotypes in response to salt, or show a different change in expression between the two genotypes. Analyses of the similarities and differences between the tolerant and sensitive lines indicated that 341 and 989 DEGs are uniquely upregulated after 6 h salt treatment in NIL-T or NIL-S, respectively; and 608 and 593 in the 3 days salt treatment (Figure 3G). We found similar values for uniquely downregulated DEGs (Figure 3H).

3.4 | GO analysis of DEGs between control and salt-treated samples of NIL-T and NIL-S

To gain insight into the putative functions of the uniquely up- and downregulated DEGs at 6 h salt treatment, the identified genes were subjected to GO (Gene Ontology) enrichment analysis, the representative GO terms are shown in Table 1, and detailed GO terms are shown in Figures S1–S4.

The enriched GO terms for the 6 h T (NIL-T) upregulated DEGs were all related to stress response such as “oxidation reduction”, “defence response” and “response to biotic stimulus” (Table 1a). Downregulated GO terms in NIL-T were less specific and mainly associated with “integral to membrane” (Table 1c). For 6 h S (NIL-S), a large number of upregulated genes were associated with the very broad GO term “regulation of transcription, DNA-dependent (GO:0006355)”, and no further downstream classification was considerably enriched (Table 1b). Downregulated GO terms in NIL-S included “heme binding”, “electron carrier activity,” “aspartic-type endopeptidase activity,” and “protein disulphide oxidoreductase activity” (Table 1d), relating to protein types instead of specific biological process GO terms.

After 3 days of salt treatment, GO analysis of uniquely up- and downregulated DEGs showed that only “oxidation reduction” and “oxidoreductase activity” were upregulated in NIL-T (Table 2a). “Oxidation reduction” and “oxidoreductase activity” were consistently upregulated in NIL-T at both time points. Table 3 shows all the 53 upregulated genes in “oxidation reduction” and “oxidoreductase activity” GO terms after 3 days treatment in NIL-T roots. A group of

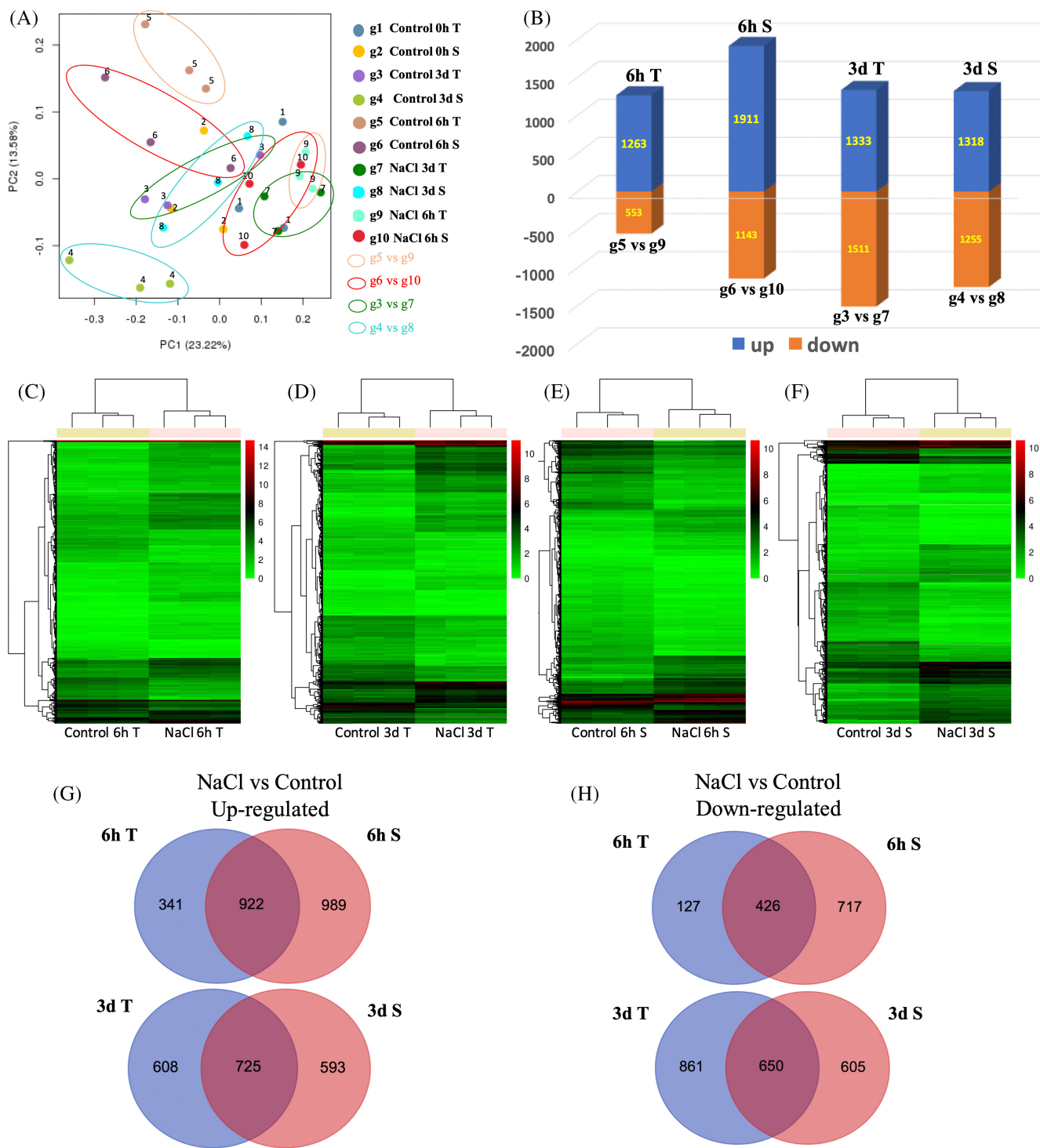


FIGURE 3 Overview of DEGs (differentially expressed genes) between salt-stressed and control samples in NIL-T and NIL-S soybeans at 6 h and 3 days. (A) PCA plot of 10 groups (g1–g10). Different coloured dots represent replicates in each group, different coloured circles represent comparisons between groups (g5 vs. g9, g6 vs. g10, g3 vs. g7, g4 vs. g8). (B) Numbers of DEGs (up and downregulated) between groups. Clustering of DEGs in log₂FPKM (fragments per Kilobase of transcript per million) of groups 3–10 (C–F). The false colour scale from green through to red indicates increasing log₂FPKM. (G) Venn diagram of upregulated DEGs in NIL-T and NIL-S soybeans at 6 h and 3 days under NaCl treatment. (H) Venn diagram of downregulated DEGs in NIL-T and NIL-S soybeans at 6 h and 3 days under NaCl treatment. The cutoffs for DEGs are Log₂FC (fold change) ≥ 1, FDR (false discover rate) < 0.01

Cytochrome P450 enzymes-encoding genes were significantly more highly expressed in NIL-T, especially *Glyma.13G173500*, which had a FPKM of 279 compared to 71 under control conditions (Table 3).

Other genes encoding oxidoreductase enzymes were also included such as peroxidases and dehydrogenases (Table 3). All the gene annotations in each GO are shown in Table S1.

TABLE 1 GO term analysis of uniquely up and downregulated genes under salt treatment in soybean roots at 6 h

GO term	Ontology	Description	Number in input list	Number in BG/ref	p value	FDR
(a)						
GO:0009607	BP	Response to biotic stimulus	7	64	9.3e−08	2.4e−05
GO:0006952	BP	Defence response	7	118	4.4e−06	0.00056
GO:0055114	BP	Oxidation reduction	28	2408	6.1e−05	0.0051
GO:0005507	MF	Copper ion binding	9	219	3.4e−06	0.00071
GO:0016491	MF	Oxidoreductase activity	32	2744	1.5e−05	0.0016
GO:0004866	MF	Endopeptidase inhibitor activity	5	92	0.00016	0.0083
(b)						
GO:0006355	BP	Regulation of transcription, DNA-dependent	69	1874	2e−05	0.0016
(c)						
GO:0016021	CC	Integral to membrane	11	1419	0.00065	0.0058
(d)						
GO:0020037	MF	Heme binding	23	728	8e−05	0.012
GO:0009055	MF	Electron carrier activity	21	702	0.00033	0.018
GO:0004190	MF	Aspartic-type endopeptidase activity	9	169	0.00042	0.018
GO:0015035	MF	Protein disulphide oxidoreductase activity	7	96	0.00031	0.018

Note: (a) Upregulated genes in NIL-T soybean roots. (b) Upregulated genes in NIL-S soybean roots. (c) Downregulated genes in NIL-T soybean roots. (d) Downregulated genes in NIL-S soybean roots.

Abbreviations: CC, cellular component; BP, biological process; MF, molecular function.

TABLE 2 GO term analysis of uniquely up and downregulated genes under salt treatment in soybean roots at 3 days

GO term	Ontology	Description	Number in input list	Number in BG/ref	p value	FDR
(a)						
GO:0055114	BP	Oxidation reduction	53	2408	8.9e−06	0.0037
GO:0016491	MF	Oxidoreductase activity	57	2744	2e−05	0.0073
(b)						
GO:0006355	BP	Regulation of transcription, DNA-dependent	51	1874	9.8e−08	3.6e−06
GO:0006468	BP	Protein amino acid phosphorylation	45	2356	0.002	0.023
GO:0048544	BP	Recognition of pollen	14	135	3.8e−09	3e−07
GO:0015743	BP	Malate transport	5	34	0.0001	0.0013
(c)						
GO:0007018	BP	Microtubule-based movement	17	155	9.8e−09	5.2e−06
GO:0003777	MF	Microtubule motor activity	17	155	9.8e−09	2.4e−06
GO:0043531	MF	ADP binding	27	467	2.1e−07	2e−05
GO:0004565	MF	Beta-galactosidase activity	6	37	9.5e−05	0.0031
GO:0017171	MF	Serine hydrolase activity	17	330	0.00014	0.0041
GO:0009341	CC	Beta-galactosidase complex	6	37	9.5e−05	0.009
(d)						
GO:0055085	BP	Transmembrane transport	29	1167	1.9e−05	0.0075
GO:0022857	MF	Transmembrane transporter activity	24	1020	0.00022	0.036

Note: (a) Upregulated genes in NIL-T soybean roots. (b) Upregulated genes in NIL-S soybean roots. (c) Downregulated genes in NIL-T soybean roots. (d) Downregulated genes in NIL-S soybean roots.

Abbreviations: CC, cellular component; BP, biological process; MF, molecular function.

TABLE 3 Upregulated genes in oxidation reduction and oxidoreductase activity GO terms of 3 days salt-treated NIL-T roots

Gmax 2.0 Protein ID	Control 3d T (FPKM)	NaCl 3d T (FPKM)	PFAM_Descriptions	Panther_Descriptions	KOG_Descriptions
<i>Glyma.13G104100</i>	0.003926	1.178719	Flavin containing amine oxidoreductase	AMINE OXIDASE	Flavin-containing amine oxidase
<i>Glyma.01G210400</i>	0.200688	2.578006	alpha/beta C-terminal domain; "lactate/malate dehydrogenase, NAD binding domain"	MALATE AND LACTATE DEHYDROGENASE	Lactate_dehydrogenase
<i>Glyma.11G024100</i>	0.040890	1.424517	Glutathione peroxidase	GLUTATHIONE PEROXIDASE	Glutathione peroxidase
<i>Glyma.13G173500</i>	71.332430	279.415321	Cytochrome P450	FAMILY NOT NAMED	Cytochrome_P450_CYP2_subfamily
<i>Glyma.02G202500</i>	0.297011	0.974227	Aldehyde dehydrogenase family	ALDEHYDE DEHYDROGENASE-RELATED	Aldehyde_dehydrogenase
<i>Glyma.18G211000</i>	1.800717	5.575660	Peroxidase	NA	NA
<i>Glyma.14G179200</i>	1.461360	2.027147	CobQ/CobB/MinD/ParA nucleotide binding domain	FAMILY NOT NAMED	Predicted_ATPase_nucleotide-binding
<i>Glyma.06G137000</i>	0.370632	1.164678	2OG-Fe(II) oxygenase superfamily	OXIDOREDUCTASE_2OG-Fe(II)_OXYGENASE_FAMILY	Iron/ascorbate_family_oxidoreductases
<i>Glyma.14G099000</i>	3.113720	7.206253	Cytokinin dehydrogenase 1, FAD and cytokinin binding; "FAD binding domain"	D-LACTATE DEHYDROGENASE	Proteins_containing_the_FAD_binding_domain
<i>Glyma.16G021200</i>	6.619380	14.499433	Cytochrome P450	FAMILY NOT NAMED	Cytochrome_P450_CYP2_subfamily
<i>Glyma.05G214000</i>	27.504467	64.849500	NAD binding domain of 6-phosphogluconate dehydrogenase	6-PHOSPHOGLUCONATE DEHYDROGENASE	6-phosphogluconate_dehydrogenase
<i>Glyma.11G175900</i>	6.988560	13.550913	Cytochrome P450	FAMILY NOT NAMED	Cytochrome_P450_CYP4/CYP19/CYP26_subfamilies
<i>Glyma.17G25700</i>	1.988862	5.125209	FAD binding domain; "Cytokinin dehydrogenase 1, FAD and cytokinin binding"	D-LACTATE DEHYDROGENASE	Proteins_containing_the_FAD_binding_domain
<i>Glyma.04G123800</i>	1.602680	3.730430	Alternative oxidase	NA	NA
<i>Glyma.19G123800</i>	0.464332	1.785490	Rubryerthrin	NA	NA
<i>Glyma.08G03800</i>	6.717425	16.957918	Flavin containing amine oxidoreductase	AMINE OXIDASE	Amine oxidase
<i>Glyma.07G168500</i>	10.873917	21.774467	2OG-Fe(II) oxygenase superfamily	OXIDOREDUCTASE_2OG-Fe(II)_OXYGENASE_FAMILY	Iron/ascorbate_family_oxidoreductases
<i>Glyma.09G132300</i>	0.903153	1.607179	CobQ/CobB/MinD/ParA nucleotide binding domain	FAMILY NOT NAMED	Predicted_ATPase_nucleotide-binding
<i>Glyma.01G056100</i>	0.352736	0.825042	2OG-Fe(II) oxygenase superfamily	OXIDOREDUCTASE_2OG-Fe(II)_OXYGENASE_FAMILY	Iron/ascorbate_family_oxidoreductases
<i>Glyma.18G177000</i>	3.027040	6.342210	Zinc-binding dehydrogenase; "Alcohol dehydrogenase GroES-like domain"	ALCOHOL DEHYDROGENASE RELATED	Alcohol_dehydrogenase_class_V
<i>Glyma.03G008100</i>	0.296423	0.491798	Cytochrome P450	FAMILY NOT NAMED	Cytochrome_P450_CYP4/CYP19/CYP26_subfamilies
<i>Glyma.05G041200</i>	0.140178	0.587665	Ferric reductase NAD binding domain; "FAD-binding domain"	NADPH OXIDASE	NA
<i>Glyma.03G098600</i>	3.067300	7.794463	Zinc-binding dehydrogenase	ALCOHOL DEHYDROGENASE RELATED	Predicted_NAD-dependent_oxidoreductase
<i>Glyma.17G167200</i>	3.817524	8.781803	FAD dependent oxidoreductase	FAD NAD BINDING OXIDOREDUCTASES	Possible_oxidoreductase
<i>Glyma.17G054500</i>	0.337715	0.774757	FAD binding domain; "Cytokinin dehydrogenase 1, FAD and cytokinin binding"	GULONOLACTONE OXIDASE	Proteins_containing_the_FAD_binding_domain
<i>Glyma.03G122000</i>	26.622283	34.891684	Cytochrome P450	FAMILY NOT NAMED	Cytochrome_P450_CYP2_subfamily
<i>Glyma.20G169200</i>	30.460700	53.630300	Peroxidase	NA	NA
<i>Glyma.11G185700</i>	6.940457	9.682720	Cytochrome P450	FAMILY NOT NAMED	Cytochrome_P450_CYP4/CYP19/CYP26_subfamilies
<i>Glyma.06G113500</i>	0.626838	1.859539	Pheophorbide a oxygenase; "Rieske [2Fe-2S] domain"	IRON-SULFUR DOMAIN CONTAINING PROTEIN	NA
<i>Glyma.15G071000</i>	14.283107	37.916700	Polyphenol oxidase middle domain; "Common central domain of tyrosinase"	TYROSINASE	NA
<i>Glyma.10G231200</i>	6.984682	16.091238	Fatty acid hydroxylase superfamily	NA	NA
<i>Glyma.10G200800</i>	1.980207	2.714897	Cytochrome P450	FAMILY NOT NAMED	Cytochrome_P450_CYP2_subfamily
<i>Glyma.15G129200</i>	8.068280	20.633733	Peroxidase	NA	NA
<i>Glyma.13G168700</i>	4.586266	11.779662	catalytic domain; "D-isomer specific 2-hydroxyacid dehydrogenase, NAD binding	2-HYDROXYACID DEHYDROGENASE-RELATED	Glyoxylate/hydroxypyruvate_reductase_(D-isomer-
<i>Glyma.10G041800</i>	0.537806	1.160858	Flavin-binding monooxygenase-like	DIMETHYLANILINE MONOOXYGENASE	Flavin-containing_monooxygenase
<i>Glyma.17G015400</i>	4.400850	6.387743	Cytochrome P450	FAMILY NOT NAMED	Cytochrome_P450_CYP2_subfamily
<i>Glyma.19G126000</i>	35.728733	48.534900	Cytochrome P450	FAMILY NOT NAMED	Cytochrome_P450_CYP2_subfamily
<i>Glyma.02G052700</i>	14.152725	29.022591	Peroxidase	NA	NA
<i>Glyma.09G218700</i>	1.588015	2.484951	High-affinity nickel-transport protein	NA	NA
<i>Glyma.06G017900</i>	12.309302	24.021127	Catalase; "Catalase-related immune-responsive"	CATALASE	Catalase
<i>Glyma.12G107000</i>	7.262499	15.171104	Pyridine nucleotide-disulphide oxidoreductase; "Pyridine nucleotide-disulphide	NADH DEHYDROGENASE-RELATED	Flavin-dehydrogenase_(ubiquinone)
<i>Glyma.11G149100</i>	0.525827	1.166289	FAD binding domain; "Cytokinin dehydrogenase 1, FAD and cytokinin binding"	GULONOLACTONE OXIDASE	Proteins_containing_the_FAD_binding_domain
<i>Glyma.20G192200</i>	0.856669	1.672531	lactate/malate dehydrogenase, alpha/beta C-terminal domain; "lactate/malate	MALATE DEHYDROGENASE	Malate_dehydrogenase
<i>Glyma.18G090700</i>	43.848325	60.982450	Glyceraldehyde 3-phosphate dehydrogenase, NAD binding domain	GLYCERALDEHYDE 3-PHOSPHATE	Glyceraldehyde_3-phosphate_dehydrogenase
<i>Glyma.06G302700</i>	12.621392	25.677667	Peroxidase	NA	NA
<i>Glyma.11G122700</i>	29.647954	50.738974	Cytochrome P450	NA	Cytochrome_P450_CYP4/CYP19/CYP26_subfamilies
<i>Glyma.05G207100</i>	36.391806	79.784041	Glutathione peroxidase	GLUTATHIONE PEROXIDASE	Glutathione_peroxidase
<i>Glyma.08G033400</i>	19.221367	37.310567	NAD binding domain of 6-phosphogluconate dehydrogenase	3-HYDROXYISOBUTYRATE DEHYDROGENASE-	Predicted_dehydrogenase
<i>Glyma.20G183100</i>	0.857535	1.409998	FAD dependent oxidoreductase	GLYCEROL-3-PHOSPHATE DEHYDROGENASE	Glycerol-3-phosphate_dehydrogenase
<i>Glyma.02G149900</i>	1.938657	3.676737	2OG-Fe(II) oxygenase superfamily	NA	Uncharacterized conserved protein
<i>Glyma.08G226600</i>	1.010831	1.571265	Complex I intermediate-associated protein 30 (CIA30); "Nmra-like family"	NAD DEPENDENT EPIMERASE/DEHYDRATASE	Predicted_dehydrogenase
<i>Glyma.14G205200</i>	91.015528	123.589510	Cytochrome P450	FAMILY NOT NAMED	Cytochrome_P450_CYP2_subfamily
<i>Glyma.15G019300</i>	25.004079	60.218292	Malic enzyme, N-terminal domain; "Malic enzyme, NAD binding domain"	MALIC ENZYME-RELATED	NADP+-dependent_malic_enzyme

Note: Annotations are achieved from <https://www.soybase.org/genomeannotation/>.

3.5 | KEGG analysis of DEGs between control and salt-treated samples

To understand what pathways were differently altered in NIL-T and NIL-S under salt stress, KEGG (Kyoto Encyclopaedia of Genes and Genomes) analysis was performed. This analysis can reveal enrichments of biological pathways, similar to GO term analysis but KEGG takes fold changes of DEGs into account, while the GO term analysis does not.

In our analysis, 1816 and 3054 DEGs in NIL-T and NIL-S, respectively, were enriched in 58 pathways (corrected *p*-value <0.05) after 6 h salt-treatment (Figure 4A). Most of the 58 pathways in both NIL-T and NIL-S were within the metabolism category with "phenylpropanoid biosynthesis," "phenylalanine metabolism," and "starch and sucrose metabolism" as the top three pathways (Figure 4A). Overall, NIL-S has more DEGs compared to NIL-T after salt-treatment, across all significantly changed pathways.

After 3 days of salt stress (3 days), 2844 and 2573 DEGs in NIL-T and NIL-S, respectively, were mapped to 57 pathways (corrected *p*-value <0.05) (Figure 4B). The metabolism category was also the most enriched after 3 days with similar pathways involved compared to 6 h. After 3 days salt-treatment, most of the significantly changed pathways included more DEGs in NIL-T compared to NIL-S, in particular in the

pathway "Protein processing in endoplasmic reticulum" (16–11 DEGs), the cell organelle where GmSALT3 is localised (Guan et al., 2014). DEG enrichment in NIL-T was also higher in the pathways "ubiquitin mediated proteolysis" (10–3 DEGs), "phenylpropanoid biosynthesis" (71–60 DEGs), "phenylalanine metabolism" (52–42 DEGs), "starch and sucrose metabolism" (43–35 DEGs), and "plant-pathogen interaction" (33–20 DEGs). It is important to note that all plants (NIL-T and NIL-S) were grown together and no plants showed signs of infection, suggesting that the genes categorised into this pathway also have a function in abiotic stress response.

In the "plant-pathogen interaction" pathway, the putative CNGC (cyclic nucleotide-gated ion channel) 15-like gene, *Glyma.13G141000*, was significantly downregulated in 3 days T (Figure S5a and S5b), and the CNGC 20-like gene, *Glyma.09G168700*, was upregulated in 3 days S. Several CaM (Calmodulin) and CML (Calmodulin-like) genes were downregulated in 3 days T. CDPK (calcium-dependent protein kinase 3, *Glyma.08G019700*) and Rboh (respiratory burst oxidase homologue protein F-like isoform 1, *Glyma.01G222700*) were upregulated in 3 days S. However, at 6 h, another CNGC 20-like gene (*Glyma.16G218300*), homologue to the Arabidopsis putative Ca²⁺ channel that is proposed to regulate cytosolic Ca²⁺ activity and expression of Rboh and CaM/CML (Demidchik et al., 2018), was significantly upregulated in NIL-T (Figure S5d).

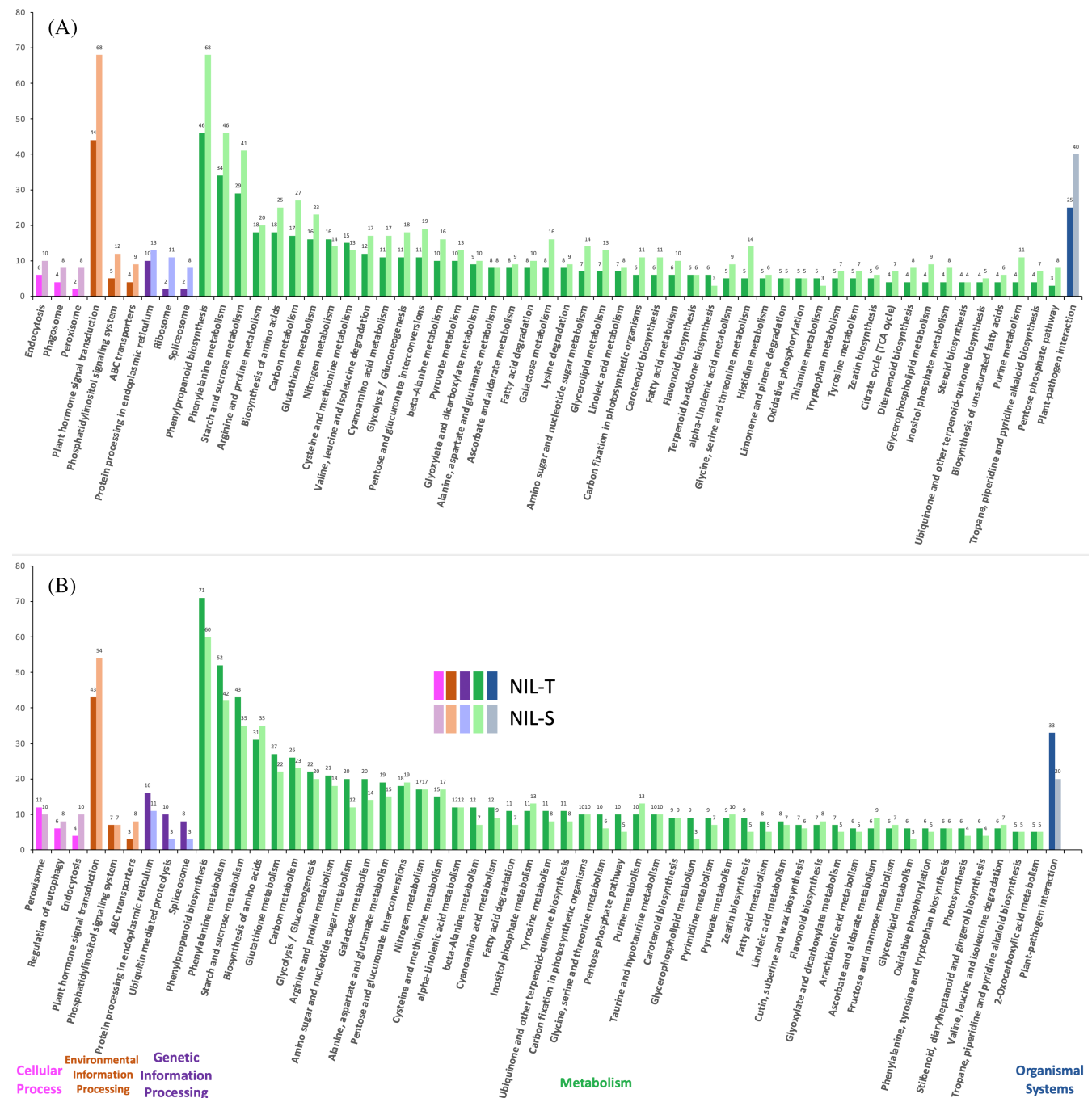


FIGURE 4 Significantly enriched KEGG (Kyoto encyclopaedia of genes and genomes) of all DEGs between salt-stressed and control samples in NIL-T and NIL-S soybeans. (A) 6 h KEGG enrichment. (B) 3 days KEGG enrichment. KEGG enrichment p -value cutoff ≤ 0.05

3.6 | Weighted gene co-expression network analysis (WGCNA)

WGCNA identifies genes that have strongly correlated expression profiles, and those genes work cooperatively in related pathways to contribute to corresponding phenotypes. It is based on the concept that genes with strongly correlated expression profiles are clustered because those genes work associatively in related pathways, contributing to the resulting phenotype; in our case, establishing salinity

tolerance after salt treatment. We applied the WGCNA to the normalised FPKM data (FPKM > 2) from all 30 RNA-seq libraries.

A co-expression network was constructed, and highly co-expressed genes were assigned to different colour-coded modules (Figure S6). Clusters were summarised by correlating the module's eigengene (or an intramodular hub gene) to the sample traits (Langfelder & Horvath, 2008). Module-trait relationships (MTRs) were computed based on Pearson's correlation between module and phenotypes, and then be used to screen modules for downstream

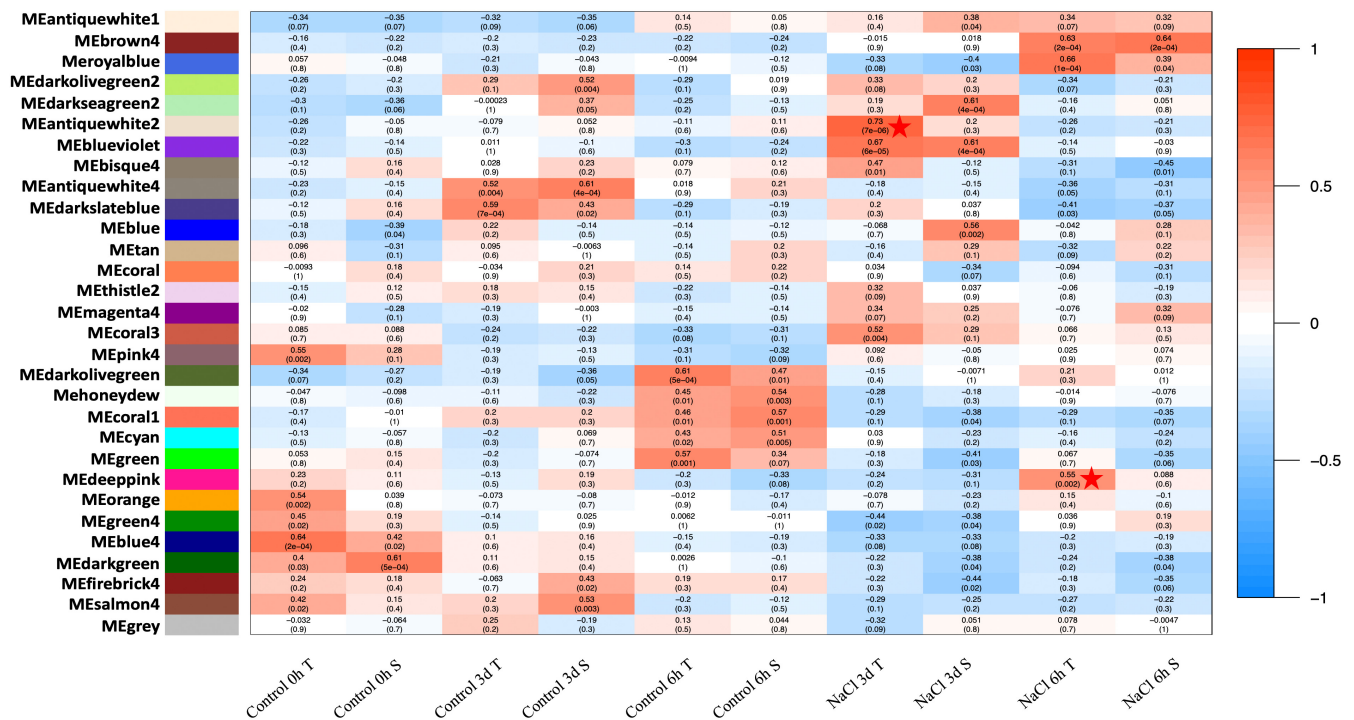


FIGURE 5 Module-trait relationships (MTRs) and corresponding *p*-values (within brackets) between the detected modules on the y-axis and groups (trait) on the x-axis. The MTRs are coloured based on their correlation: from red (strong positive correlation) to blue (strong negative correlation). Each group contains three biological replicates. Pentagram represents modules of interest

TABLE 4 Significant gene ontology (GO) terms in MEdeppink and MEantiquewhite2 modules

GO term	Ontology	Description	Number in input list	Number in BG/ref	<i>p</i> value	FDR
(a)						
GO:0005886	C	Plasma membrane	12	81	5.00e−20	1.70e−18
GO:0031224	C	Intrinsic to membrane	12	1453	4.40e−06	4.90e−05
GO:0016021	C	Integral to membrane	12	1419	3.50e−06	4.90e−05
GO:0044425	C	Membrane part	13	1801	7.00e−06	5.80e−05
GO:0016020	C	Membrane	15	3518	0.00053	0.0035
(b)						
GO:0009207	P	Purine ribonucleoside triphosphate catabolic process	6	40	0.0000092	0.00044
GO:0046907	P	Intracellular transport	14	297	0.0000073	0.00044
GO:0016567	P	Protein ubiquitination	9	130	0.000019	0.00076
GO:0046034	P	ATP metabolic process	5	46	0.00021	0.0046
GO:0046578	P	Regulation of Ras protein signal transduction	6	91	0.00061	0.011
GO:0004674	F	Protein serine/threonine kinase activity	14	39	3.1e−16	1.2E-13
GO:0046872	F	Metal ion binding	65	3600	0.000024	0.0021
GO:0042623	F	ATPase activity, coupled	12	343	0.00047	0.021
GO:0030120	C	Vesicle coat	5	41	0.00013	0.0013
GO:0031981	C	Nuclear lumen	5	105	0.0066	0.039
GO:0016021	C	Integral to membrane	26	1419	0.0068	0.039

Note: (a) Enriched GO terms in MEdeppink module (NIL-T after 6 h salt treatment); (b) enriched GO terms in MEantiquewhite2 module (NIL-T after 3 days salt treatment).

Abbreviations: C, cellular component; P, biological process; F, molecular function.

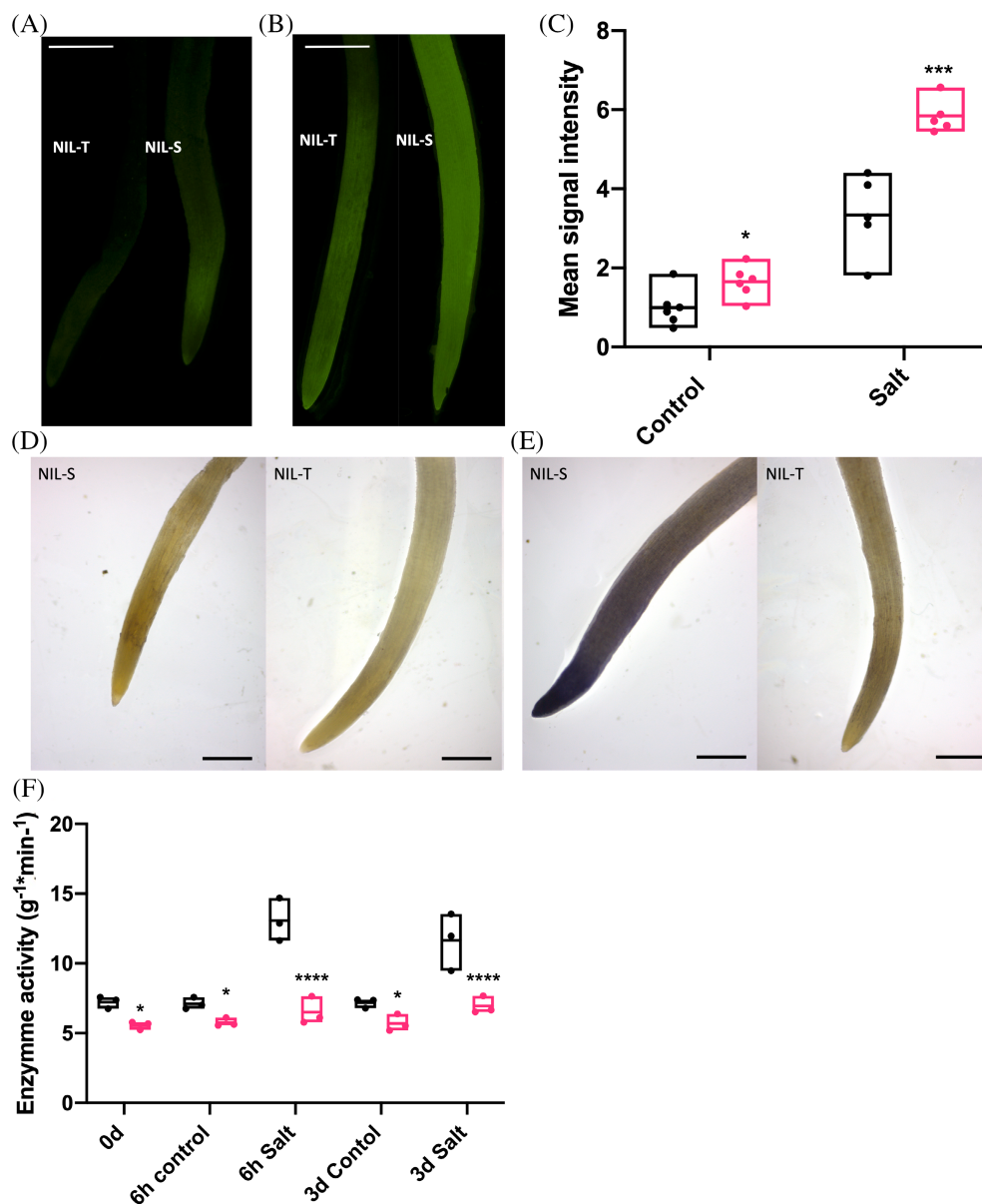


FIGURE 6 ROS production and enzyme activity of the superoxide anion (O_2^-) scavenger assay in soybean roots. NIL-T and NIL-S were labelled with 30 μ M DCFDA for 10 min under control conditions (A) and with 200 mM NaCl salt treatment for 3 days (B). Bar = 1000 μ m. Green fluorescence indicates the presence of ROS, and the mean signal intensity (C) was measured using ImageJ, asterisk indicates a significant difference between NIL-T and NIL-S at $**p < 0.001$, $***p < 0.0001$, $n = 5-6$. NBT staining indicates the superoxide content of the root tips of NIL-T and NIL-S under control conditions (D) and with 200 mM NaCl salt treatment for 3 days (E), the staining intensity reflects the concentration of superoxide. Bar = 1 mm. (F) Scavenging activity of the superoxide anion (O_2^-) of NIL-T (black) and NIL-S (pink) with or without salt treatment. Asterisk indicates a significant difference between NIL-T and NIL-S at $*p < 0.05$, $***p < 0.0001$, $n = 3$.

analysis. Thirty clusters of highly co-expressed genes (modules) were detected and are shown in differently coloured module (Figure 5). To investigate what genes show strongly correlated co-expression in NIL-T under saline conditions (6 h and 3 days), two modules of interest were selected for functional annotation based on their correlation value and corresponding p value. One module contains 79 genes that show strongly correlated co-expression in NIL-T after 6 h salt treatment; this model is depicted here in a shade of pink (MEdeppink). The second selected module, colour-coded here in a shade of white (MEantiquewhite2), contains 406 genes which expression profiles are highly correlated in NIL-T after 3 days salt treatment.

GO analysis of 79 genes in module MEdeppink is shown in Table 4a; GO analysis of 406 genes in module MEantiquewhite2 is shown in Table 4b. Within the highly co-expressed 79 genes in NIL-T after 6 h salt treatment (MEdeppink module), Gene Ontology (GO) analysis indicates 12 of them are integral to plasma membrane (GO:0016021; Table 4a), and they encode a group of Casparian strip

membrane proteins (Table S1). Highly co-expressed 406 genes in NIL-T after 3 days salt treatment (MEantiquewhite2 module) are enriched in GO:0016021 (integral to membrane; 26 genes), which are related to intracellular vesicle trafficking and ion transport (Table 4b). Within those GOs, there are genes relevant to vesicle transport, such as genes encoding for coatamer subunits and transmembrane protein transporters; three potassium transporters including Glyma.05g213100 (TRH1; tiny root hair 1), Glyma.08g288500 (KUP6; potassium ion uptake transporter 6), and Glyma.13g170700 (Table S1).

3.7 | RT-qPCR validation for RNA-seq results

In order to confirm the RNA-seq results, 10 DEGs were selected for RT-qPCR validation based on their RPKM transcript abundance. Importantly, this occurred on independently grown plants not used for RNAseq analysis but grown in identical conditions. RT-qPCR

indicated that relative expression values (relative to housekeeping gene *GmUKN1*) of the selected DEGs were significantly correlated with their FPKM values (Figure S7).

3.8 | ROS production and scavenger enzymes activity

Due to the enrichment of the “Oxidation reduction” gene ontology category in NIL-T plants under salt (Table 3), we decided to test if this translated into a difference in ROS generation or detoxification in NIL-T compared to NIL-S, again on independently grown plants. The ROS activity was measured in the roots of NIL-T and NIL-S after a 3-day with or without salt treatment, using a fluorescent dye (Figure 6A and B). We could detect a lower ROS activity in NIL-T compared to NIL-S roots, already in the control conditions, consistent with the expression of *GmSALT3* under control conditions. This difference strongly increased when comparing plants from saline conditions; ROS were strongly produced in NIL-S under salt treatment. The quantified fluorescence intensity of staining confirmed that under both control and salt treatment, NIL-T could maintain a significantly lower ROS content in the roots (Figure 6C).

ROS are composed of many different molecules; we initially measured the concentration of the ROS H_2O_2 . We could detect a higher H_2O_2 concentration in both lines under salt treatment compared to control; but no concentration differences between NIL-T and NIL-S in either control or salt treatment could be measured (Figure S9), suggesting that the increase in ROS is attributed to a different molecule. Therefore, we used Nitroblue tetrazolium (NBT) to measure the production of ROS superoxide, and the results (Figure 6D and E) showed that the staining intensity was much weaker in the NIL-T than NIL-S after 3 days salt treatment, which indicates NIL-T accumulated lower concentrations of superoxide than NIL-S in the roots. The antioxidant properties of the roots of NIL-T and NIL-S with or without salt treatment was then analysed using guaiacol. The antioxidant enzyme activity was assayed by measuring the absorbance at 470 nm due to the enzyme dependent oxidation of guaiacol by H_2O_2 (Pi et al., 2016). The scavenging enzyme activity of the superoxide anion was significantly higher in NIL-T compared to NIL-S under control and saline conditions (Figure 6F).

4 | DISCUSSION

Soybean cultivars harbouring *GmSALT3* are better able to modulate Na^+ , K^+ , and Cl^- content of shoots under salinity (Do et al., 2016; Guan et al., 2014; Liu et al., 2016; Qi et al., 2014; Qu et al., 2021), and they have a yield advantage under saline conditions compared to soybean varieties without a functional *GmSALT3* (Do et al., 2016; Liu et al., 2016). The *GmSALT3* ion transport protein is ER-localised (Guan et al., 2014), suggesting a cellular function of *GmSALT3* that is not directly connected to ion uptake or exclusion. We performed detailed and extended RNAseq analysis of NIL-T and NIL-S soybeans

to decipher the cellular pathways and processes that connect *GmSALT3* to soybean salinity tolerance. We could identify several genes and biological pathways involved in responses to salt stress in *GmSALT3*-containing NIL-T plants, which gives an insight into how *GmSALT3* expression translates into a phenotype through modulating cell processes.

Illumina sequencing results showed that all the 30 constructed RNA-seq libraries were of sufficient quality for further analysis. On average the RNA-seq libraries had 26.8 million clean mapped reads, and reads were mapped to 53,625 annotated soybean genes with 353 additional transcripts not previously annotated—probably due to the germplasm being genetically divergent from the reference. Minimal DEGs could be detected between NIL-T and NIL-S at 0 h, 6 h, and 3 days under control conditions (Figure 2), this indicates that NIL-T and NIL-S roots had similar gene expression patterns under non-stressed conditions. In the three consistently upregulated DEGs in NIL-S at all time points under control conditions, there was a gene encoding for a LOX (Linoleate 13S-lipoxygenase 3-1) (Figure 2C). Lipoxygenases (LOXs) are involved in defence responses against biotic stresses, such as microbial pathogens and insect pests, in tomato (Hu et al., 2015), potato (Royo et al., 1999), maize (Gao et al., 2009), and rice (Zhou et al., 2009). The full length *GmSALT3* during soybean natural selection and domestication was lost several times independently (Guan et al., 2014), suggesting that plants with a non-functional *GmSALT3* might have a benefit when grown under non-saline conditions. This benefit might be related to higher LOXs expression in soybean cultivars harbouring the sensitive alleles, which could be beneficial under certain biotic stresses. In potato, depletion of one specific LOX (LOX-H3) negatively affected their response to stress (Royo et al., 1999), but here in soybean, plants with the full length *GmSALT3* had lower LOX expression than with the non-functional *GmSALT3*. Loss of *GmSALT3* function appears to occur in non-saline regions so this might confer an advantage to the plant under some conditions (Guan et al., 2014). It is possible that greater LOX expression in soybean confers an advantage in certain conditions not studied here, such as biotic stress, which could be an area of further study.

Comparing DEGs, the GO terms “oxidation reduction (GO:0055114)” and “oxidoreductase activity (GO:0016491)” were consistently upregulated in NIL-T at 6 h and 3 days of salt treatment, with a greater number of genes in this term upregulated after 3 days, which indicates that NIL-T plants may have a greater capacity to detoxify ROS (reactive oxygen species) than NIL-S plants. We could experimentally confirm this and show that more ROS are present in NIL-S roots compared to NIL-T (Figure 6A–E) and NIL-T possessed a significantly higher scavenging enzyme activity of the superoxide anion (O_2^-) (Figure 6F). Phenylalanine is the precursor for flavonoids, and flavonoids are utilised to scavenge and protect against ROS (Dastmalchi et al., 2016). The increase in gene expression related to phenylalanine synthesis seen in NIL-T (Figure 4A and B) is consistent with the observation that *GmSALT3* is connected to an increase in general ROS detoxification capacity. ROS detoxification and signalling is frequently linked to improvements in stress tolerance in plants (Dong et al., 2013; Munns & Gilliam, 2015; Munns & Tester, 2008;

Roy et al., 2014). For instance, the exogenous application of scavengers such as the non-enzymatic antioxidant ascorbic acid has previously improved plant performance under stress (Akram et al., 2017), but such treatments are impractical in the field and are likely to have additional impact on the plant and microbial communities as a carbon source. Here, the expression of *GmSALT3* is correlated with the ability to detoxify ROS, and therefore represents an upstream genetic mechanism likely to enhance this capacity over germplasm not expressing *GmSALT3*.

In all the listed upregulated genes in NIL-T (Table 3), a group of Cytochrome P450 enzymes-coding genes were significantly more highly expressed in NIL-T in response to salt-treatment, especially *Glyma.13G173500*, which has the highest expression level and a fold change of 3.93. The cytochrome P450 (CYP) family is a large and essential protein superfamily in plants, and CYPs catalyse mono-oxygenation/hydroxylation reactions in primary and secondary metabolism pathways (Mizutani & Ohta, 2010). NaCl can induce conformational change of cytochrome P450 in animals (Oyekan et al., 1999; Yun et al., 1996), but this has not been investigated in plants. In soybean, there are 322 identified CYPs, with only few of them having been functionally characterised (Guttikonda et al., 2010). *GmCYP82A3* (*Glyma.13g068800*) (Yan et al., 2016) and *GmCYP51G1* (*Glyma.07g110900*) (Pi et al., 2016) were shown to be involved in plant tolerance stresses such as salinity and drought. The two P450 containing isoflavone synthases (IFS) *GmIFS1* (*Glyma.07G202300*) and *GmIFS2* (*GmCYP93C1 = Glyma.13G173500*) are both anchored in the ER, the same organelle where *GmSALT3* is localised. *GmIFS2* is a DEG identified in our study. Expression of *GmIFS1* was previously shown to be induced by salt stress, and has been linked to improving salinity tolerance through the accumulation of isoflavone content (Jia et al., 2017). We found its homologue, *GmIFS2* (*Glyma.13G173500*), had a fold change of 3.93 in NIL-T in response to salt stress (Table 3). Combined, this suggests that the function of *GmSALT3* could be important for the synthesis of isoflavones, and this may contribute to salt tolerance.

ROS production has been linked to Ca^{2+} influx into cells and specifically the activity of CNGCs (Ma et al., 2009). Ca^{2+} and ROS act as signalling molecules when plant roots are suddenly exposed to salt (Byrt et al., 2018; Stephan & Schroeder, 2014). Gene expression related to proposed Ca^{2+} signalling elements are different between NIL-T and NIL-S. As a result, our analysis suggested that the “plant–pathogen interaction” pathway could be highly activated in NIL-S, which may lead to higher ROS production and hypersensitive responses (Figure S5a and c). Under 6 h salt treatment, several CNGCs were also significantly upregulated in NIL-S, which may relate to activation of different signalling cascades (Figure S5d). Several CaM (calmodulin) and CML (Calmodulin-like) genes are also downregulated in 3 days T (Figure S5b), downregulation of CaM and CML may have been proposed to restrict gaseous reactive oxygen species (ROS) production in plants (Ma & Berkowitz, 2011).

The WGCNA analysis revealed that genes related to Casparian strip (CS) development were upregulated in NIL-T within 6 h of salt treatment. CSs play an important role in regulating nutrient uptake

and salt stress tolerance, as they form the diffusion barrier for ions into the stele (Chen et al., 2011; Roppolo et al., 2011). CS localised membrane proteins (CASPs) were shown to mediate CS formation in Arabidopsis, by guiding the local lignin deposition during cell wall modification (Roppolo et al., 2011). Upon immobilisation, CASPs recruit PER64 (Peroxidase 64), RBOHF (respiratory burst oxidase Homologue F), ESB1 (enhanced suberin 1), and dirigent proteins, to establish the lignin polymerisation system (Hosmani et al., 2013; Kamiya et al., 2015; Lee et al., 2013). Our analysis identified a module of genes upregulated under salt exclusively in the NIL-T (MKdeppink module). This module contains eight dirigent genes, peroxidase 64 (*Glyma.14g221400*) as well as CASPs. The combination of genes in this model suggests that NIL-T plants might more efficiently induce an earlier formation of the endodermal diffusion barrier as well as the formation of an exodermal diffusion barrier, in response to salt stress. We stained lignin and suberin in NIL-T and NIL-S roots with ClearSee and Auramine O, following the protocol developed by Ursache et al. (2018), in order to compare the CS development. Unfortunately, we could only observe autofluorescence in both NIL-T and NIL-S root differentiation zone that close to the root tips using confocal microscopy. So the link between *GmSALT3* and CS formation needs further validation.

Lastly, CHX transporters (of which *GmSALT3* is a member) were shown to be associated with the endocytic and exocytic pathways in dynamic endomembrane system (Chanroj et al., 2012; Padmanaban et al., 2007). Our results and the previously proposed vesicle trafficking function of CHXs (Chanroj et al., 2012), suggests that *GmSALT3* might be important for establishing optimal conditions in the ER lumen, which could subsequently impact the secretion of compounds such as signalling molecules, ions, and soluble proteins.

To summarise, our findings suggest that the *GmSALT3* containing NIL-T has a higher salinity tolerance because NIL-T roots are more effective in detoxifying ROS, potentially through ER-localised flavonoid biosynthesis enzymes, which helps to prevent cellular damage. Additionally, our study has identified that Ca^{2+} signalling, vesicle trafficking and Casparian strip development might be modulated by *GmSALT3*, and are therefore areas for further study.

AUTHOR CONTRIBUTIONS

MG, YQ and RG designed experiments, with input from SW and LQ. Yue Qu and Rongxia Guan analysed the data. Lijuan Qiu and Matthew Gilliam directed the project. Oliver Berkowitz and James Whelan contributed to RNA-sequencing. Lili Yu performed plant samples harvest for RNA-sequencing. Rakesh David contributed to RNA-sequencing analysis. Yue Qu, Matthew Gilliam and Rongxia Guan wrote the paper. Stefanie Wege and Lijuan Qiu assisted in editing the final version of the manuscript. All authors commented on the manuscript.

ACKNOWLEDGMENTS

This work was funded by the Natural Science Foundation of China, grant number 31830066 (RG); Scientific Innovation Project of Chinese Academy of Agricultural Sciences (L-J Q). YQ and SH were supported

by Australian Research Council Centre of Excellence funding awarded to MG (CE140100008). Australian Research Council Fellowships supported MG (FT130100709) and SW (DE160100804). We thank Na Sai and Dr. Miriam Schreiber for assisting in WGCNA analysis. Open access publishing facilitated by The University of Adelaide, as part of the Wiley - The University of Adelaide agreement via the Council of Australian University Librarians. Open access publishing facilitated by The University of Adelaide, as part of the Wiley - The University of Adelaide agreement via the Council of Australian University Librarians.

CONFLICT OF INTEREST

The authors declare that they have no conflict of interest.

DATA AVAILABILITY STATEMENT

The data supporting the findings of this study are available from the corresponding author, Matthew Gilliham, upon request.

ORCID

Yue Qu  <https://orcid.org/0000-0003-0101-1097>

Rongxia Guan  <https://orcid.org/0000-0002-6826-9239>

Oliver Berkowitz  <https://orcid.org/0000-0002-7671-6983>

James Whelan  <https://orcid.org/0000-0001-5754-025X>

Stefanie Wege  <https://orcid.org/0000-0002-7232-5889>

Matthew Gilliham  <https://orcid.org/0000-0003-0666-3078>

REFERENCES

- Aghaei, K., Ehsanpour, A., Shah, A. & Komatsu, S. (2009) Proteome analysis of soybean hypocotyl and root under salt stress. *Amino Acids*, 36, 91–98.
- Akram, N.A., Shafiq, F. & Ashraf, M. (2017) Ascorbic acid—a potential oxidant scavenger and its role in plant development and abiotic stress tolerance. *Frontiers in Plant Science*, 8, 613.
- Andrews, S. (2010) FastQC: a quality control tool for high throughput sequence data. <http://www.bioinformatics.babraham.ac.uk/projects/fastqc/>.
- Bose, J., Rodrigo-Moreno, A. & Shabala, S. (2014) ROS homeostasis in halophytes in the context of salinity stress tolerance. *Journal of Experimental Botany*, 65, 1241–1257.
- Byrt, C.S., Munns, R., Burton, R.A., Gilliham, M. & Wege, S. (2018) Root cell wall solutions for crop plants in saline soils. *Plant Science*, 269, 47–55.
- Chanroj, S., Wang, G., Venema, K., Zhang, M.W., Delwiche, C.F. & Sze, H. (2012) Conserved and diversified gene families of monovalent cation/H⁺ antiporters from algae to flowering plants. *Frontiers in Plant Science*, 3, 25.
- Chen, T., Cai, X., Wu, X., Karahara, I., Schreiber, L. & Lin, J. (2011) Casparian strip development and its potential function in salt tolerance. *Plant Signaling & Behavior*, 6(10), 1499–1502.
- Choudhury, F.K., Rivero, R.M., Blumwald, E. & Mittler, R. (2017) Reactive oxygen species, abiotic stress and stress combination. *The Plant Journal* 90, 856–867.
- Dastmalchi, M., Bernards, M.A. & Dhaubhadel, S. (2016) Twin anchors of the soybean isoflavonoid metabolon: evidence for tethering of the complex to the endoplasmic reticulum by IFS and C4H. *The Plant Journal*, 85, 689–706.
- Demidchik, V., Shabala, S., Isayenkov, S., Cuin, T.A. & Pottosin, I. (2018) Calcium transport across plant membranes: mechanisms and functions. *New Phytologist*, 220(1), 49–69.
- Do, T.D., Chen, H., Hien, V.T.T., Hamwieh, A., Yamada, T., Sato, T. et al. (2016) Ncl synchronously regulates Na⁺, K⁺, and Cl⁻ in soybean and greatly increases the grain yield in saline field conditions. *Scientific Reports*, 6, 19147.
- Dong, W., Wang, M., Xu, F., Quan, T., Peng, K., Xiao, L. et al. (2013) Wheat oxophytodienoate reductase gene *TaOPR1* confers salinity tolerance via enhancement of abscisic acid signaling and reactive oxygen species scavenging. *Plant Physiology*, 161, 1217–1228.
- Du, Z., Zhou, X., Ling, Y., Zhang, Z. & Su, Z. (2010) agriGO: a GO analysis toolkit for the agricultural community. *Nucleic Acids Research*, 38, 64–70.
- Flowers, T.J., Galal, H.K. & Bromham, L. (2010) Evolution of halophytes: multiple origins of salt tolerance in land plants. *Functional Plant Biology*, 37, 604–612.
- Foreman, J., Demidchik, V., Bothwell, J.H., Mylona, P., Miedema, H., Torres, M.A. et al. (2003) Reactive oxygen species produced by NADPH oxidase regulate plant cell growth. *Nature*, 422, 442–446.
- Foyer, C.H. & Noctor, G. (2005) Redox homeostasis and antioxidant signaling: a metabolic interface between stress perception and physiological responses. *Plant Cell*, 17, 1866–1875.
- Gao, X., Brodhagen, M., Isakeit, T., Brown, S.H., Göbel, C., Betran, J. et al. (2009) Inactivation of the lipoxygenase *ZmLOX3* increases susceptibility of maize to *Aspergillus* spp. *Molecular Plant Microbe Interactions*, 22, 222–231.
- Ge, Y., Li, Y., Zhu, Y.-M., Bai, X., Lv, D.-K., Guo, D. et al. (2010) Global transcriptome profiling of wild soybean (*Glycine soja*) roots under NaHCO₃ treatment. *BMC Plant Biology*, 10, 153.
- Gill, S.S. & Tuteja, N. (2010) Reactive oxygen species and antioxidant machinery in abiotic stress tolerance in crop plants. *Plant Physiology and Biochemistry*, 48, 909–930.
- Gilliham, M., Able, J.A. & Roy, S.J. (2017) Translating knowledge about abiotic stress tolerance to breeding programmes. *The Plant Journal*, 90, 898–917.
- Grant, D., Nelson, R.T., Cannon, S.B. & Shoemaker, R.C. (2010) SoyBase, the USDA-ARS soybean genetics and genomics database. *Nucleic Acids Research*, 38(Suppl. 1), D843–D846.
- Guan, R., Qu, Y., Guo, Y., Yu, L., Liu, Y., Jiang, J. et al. (2014) Salinity tolerance in soybean is modulated by natural variation in *GmSALT3*. *The Plant Journal*, 80, 937–950.
- Guttikonda, S.K., Trupti, J., Bisht, N.C., Chen, H., An, Y.-Q.C., Pandey, S. et al. (2010) Whole genome co-expression analysis of soybean cytochrome P450 genes identifies nodulation-specific P450 monooxygenases. *BMC Plant Biology*, 10, 243.
- Hosmani, P.S., Kamiya, T., Danku, J., Naseer, S., Geldner, N., Guerinot, M.L. et al. (2013) Dirigent domain-containing protein is part of the machinery required for formation of the lignin-based Casparian strip in the root. *Proceedings of the National Academy of Sciences*, 110(35), 14498–14503.
- Hu, R., Fan, C., Li, H., Zhang, Q. & Fu, Y.F. (2009) Evaluation of putative reference genes for gene expression normalization in soybean by quantitative real-time RT-PCR. *BMC Molecular Biology*, 10, 93.
- Hu, T., Hu, Z., Zeng, H., Qv, X. & Chen, G. (2015) Tomato lipoxygenase D involved in the biosynthesis of jasmonic acid and tolerance to abiotic and biotic stress in tomato. *Plant Biotechnology Reports*, 9, 37–45.
- Jia, T., An, J., Liu, Z., Yu, B. & Chen, J. (2017) Salt stress induced soybean *GmIFS1* expression and isoflavone accumulation and salt tolerance in transgenic soybean cotyledon hairy roots and tobacco. *Plant Cell, Tissue and Organ Culture (PCTOC)*, 128, 469–477.
- Kamiya, T., Borghi, M., Wang, P., Danku, J.M., Kalmbach, L., Hosmani, P.S. et al. (2015) The MYB36 transcription factor orchestrates Casparian strip formation. *Proceedings of the National Academy of Sciences*, 112(33), 10533–10538.
- Kanehisa, M., Araki, M., Goto, S., Hattori, M., Hirakawa, M., Itoh, M. et al. (2007) KEGG for linking genomes to life and the environment. *Nucleic Acids Research*, 36, D480–D484.
- Kim, D., Perteau, G., Trapnell, C., Pimentel, H., Kelley, R. & Salzberg, S.L. (2013) TopHat2: accurate alignment of transcriptomes in the presence of insertions, deletions and gene fusions. *Genome Biology*, 14, R36.

- Lam, H.M., Xu, X., Liu, X., Chen, W., Yang, G., Wong, F.L. et al. (2010) Resequencing of 31 wild and cultivated soybean genomes identifies patterns of genetic diversity and selection. *Nature Genetics*, 42, 1053–1059.
- Langfelder, P. & Horvath, S. (2008) WGCNA: an R package for weighted correlation network analysis. *BMC Bioinformatics*, 9(1), 559.
- Langfelder, P., Zhang, B. & Horvath, S. (2008) Defining clusters from a hierarchical cluster tree: the dynamic tree cut package for R. *Bioinformatics*, 24(5), 719–720.
- Lee, Y., Rubio, M.C., Alassimone, J. & Geldner, N. (2013) A mechanism for localized lignin deposition in the endodermis. *Cell*, 153(2), 402–412.
- Liu, Y., Yu, L., Qu, Y., Chen, J., Liu, X., Hong, H. et al. (2016) GmSALT3, which confers improved soybean salt tolerance in the field, increases leaf Cl^- exclusion prior to Na^+ exclusion but does not improve early vigor under salinity. *Frontiers in Plant Science*, 7, 1485.
- Li, S., Wang, N., Ji, D., Zhang, W., Wang, Y., Yu, Y. et al. (2019) A GmSIN1/GmNCE3s/GmRbohBs feed-forward loop acts as a signal amplifier that regulates root growth in soybean exposed to salt stress. *The Plant Cell*, 31(9), 2107–2130.
- Lu, Y., Lam, H., Pi, E., Zhan, Q., Tsai, S., Wang, C. et al. (2013) Comparative metabolomics in *Glycine max* and *Glycine soja* under salt stress to reveal the phenotypes of their offspring. *Journal of Agricultural and Food Chemistry*, 61, 8711–8721.
- Ma, W. & Berkowitz, G.A. (2011) Ca^{2+} conduction by plant cyclic nucleotide gated channels and associated signaling components in pathogen defense signal transduction cascades. *New Phytologist*, 190, 566–572.
- Ma, W., Smigel, A., Verma, R. & Berkowitz, G.A. (2009) Cyclic nucleotide gated channels and related signaling components in plant innate immunity. *Plant Signaling & Behavior*, 4, 277–282.
- Mao, X., Cai, T., Olyarchuk, J.G. & Wei, L. (2005) Automated genome annotation and pathway identification using the KEGG Orthology (KO) as a controlled vocabulary. *Bioinformatics*, 21, 3787–3793.
- Mittler, R. (2002) Oxidative stress, antioxidants and stress tolerance. *Trends in Plant Science*, 7, 405–410.
- Mittler, R., Vanderauwera, S., Gollery, M. & Van Breusegem, F. (2004) Reactive oxygen gene network of plants. *Trends in Plant Science*, 9, 490–498.
- Mizutani, M. & Ohta, D. (2010) Diversification of P450 genes during land plant evolution. *Annual Review of Plant Biology*, 61, 291–315.
- Munns, R. & Gilliam, M. (2015) Salinity tolerance of crops—what is the cost? *New Phytologist*, 208, 668–673.
- Munns, R. & Tester, M. (2008) Mechanisms of salinity tolerance. *Annual Review of Plant Biology*, 59, 651–681.
- Neill, S., Desikan, R. & Hancock, J. (2002) Hydrogen peroxide signalling. *Current Opinion in Plant Biology*, 5, 388–395.
- Noctor, G. & Foyer, C.H. (1998) Ascorbate and glutathione: keeping active oxygen under control. *Annual Review of Plant Biology*, 49, 249–279.
- Overmyer, K., Brosché, M. & Kangasjärvi, J. (2003) Reactive oxygen species and hormonal control of cell death. *Trends in Plant Science*, 8, 335–342.
- Oyekan, A., Youseff, T., Fulton, D., Quilley, J. & McGiff, J. (1999) Renal cytochrome P450 ω -hydroxylase and epoxygenase activity are differentially modified by nitric oxide and sodium chloride. *Journal of Clinical Investigation*, 104, 1131–1137.
- Padmanaban, S., Chanroj, S., Kwak, J.M., Li, X., Ward, J.M. & Sze, H. (2007) Participation of endomembrane cation/ H^+ exchanger AtCHX20 in osmoregulation of guard cells. *Plant Physiology*, 144(1), 82–93.
- Pei, Z.M., Murata, Y., Benning, G., Thomine, S., Klüsener, B., Allen, G.J. et al. (2000) Calcium channels activated by hydrogen peroxide mediate abscisic acid signalling in guard cells. *Nature*, 406, 731–734.
- Pi, E., Qu, L., Hu, J., Huang, Y., Qiu, L., Lu, H. et al. (2016) Mechanisms of soybean roots' tolerances to salinity revealed by proteomic and phosphoproteomic comparisons between two cultivars. *Molecular & Cellular Proteomics*, 15, 266–288.
- Prakash, D., Niranjana, A., Tewari, S.K. & Pushpangadan, P. (2001) Underutilised legumes: potential sources for low-cost protein. *International Journal of Food Sciences and Nutrition*, 52, 337–341.
- Qi, X., Li, M.W., Xie, M., Liu, X., Ni, M., Shao, G. et al. (2014) Identification of a novel salt tolerance gene in wild soybean by whole-genome sequencing. *Nature Communications*, 5, 4340.
- Qin, J., Gu, F., Liu, D., Yin, C., Zhao, S., Chen, H. et al. (2013) Proteomic analysis of elite soybean Jidou17 and its parents using iTRAQ-based quantitative approaches. *Proteome Science*, 11, 12.
- Qu, Y., Guan, R., Bose, J., Henderson, S.W., Wege, S., Qiu, L. et al. (2021) Soybean CHX-type ion transport protein GmSALT3 confers leaf Na^+ exclusion via a root derived mechanism, and Cl^- exclusion via a shoot derived process. *Plant Cell & Environment*, 44, 856–869.
- Roppolo, D., De Rybel, B., Tendon, V.D., Pfister, A., Alassimone, J., Vermeer, J.E. et al. (2011) A novel protein family mediates Casparian strip formation in the endodermis. *Nature*, 473(7347), 380–383.
- Roy, S.J., Negrão, S. & Tester, M. (2014) Salt resistant crop plants. *Current Opinion in Biotechnology*, 26, 115–124.
- Royo, J., León, J., Vancanney, G., Albar, J.P., Rosahl, S., Ortego, F. et al. (1999) Antisense-mediated depletion of a potato lipoxygenase reduces wound induction of proteinase inhibitors and increases weight gain of insect pests. *Proceedings of the National Academy of Sciences*, 96, 1146–1151.
- Schindelin, J., Arganda-Carreras, I., Frise, E., Kaynig, V., Longair, M., Pietzsch, T. et al. (2012) Fiji: an open-source platform for biological-image analysis. *Nature Methods*, 9(7), 676–682.
- Sharma, M., Gupta, S.K., Deeba, F. & Pandey, V. (2017) Effects of reactive oxygen species on crop productivity: an overview. In: Singh, V.P., Singh, S., Tripathi, D.K., Prasad, S.M. & Chauhan, D.K. (Eds.) *Revisiting the role of ROS in plants: boon or bane - revisiting the role of ROS*. Chapter 6. Chichester, England: John Wiley & Sons Ltd.
- Stephan, A.B. & Schroeder, J.I. (2014) Plant salt stress status is transmitted systemically via propagating calcium waves. *Proceedings of the National Academy of Sciences*, 111(17), 6126–6127.
- Toorchi, M., Yukawa, K., Nouri, M.-Z. & Komatsu, S. (2009) Proteomics approach for identifying osmotic-stress-related proteins in soybean roots. *Peptides*, 30, 2108–2117.
- Trapnell, C., Roberts, A., Goff, L., Pertea, G., Kim, D., Kelley, D.R. et al. (2012) Differential gene and transcript expression analysis of RNA-seq experiments with TopHat and Cufflinks. *Nature Protocols*, 7, 562–578.
- Ursache, R., Andersen, T.G., Marhavý, P. & Geldner, N. (2018) A protocol for combining fluorescent proteins with histological stains for diverse cell wall components. *The Plant Journal*, 93, 399–412.
- Yan, Q., Cui, X., Lin, S., Gan, S., Xing, H. & Dou, D. (2016) GmCYP82A3, a soybean cytochrome P450 family gene involved in the jasmonic acid and ethylene signaling pathway, enhances plant resistance to biotic and abiotic stresses. *PLoS One*, 11, e0162253.
- Yun, C.H., Song, M., Ahn, T. & Kim, H. (1996) Conformational change of cytochrome P450 1A2 induced by sodium chloride. *Journal of Biological Chemistry*, 271, 31312–31316.
- Zhou, G., Qi, J., Ren, N., Cheng, J., Erb, M., Mao, B. et al. (2009) Silencing OsHI-LOX makes rice more susceptible to chewing herbivores, but enhances resistance to a phloem feeder. *The Plant Journal*, 60, 638–648.

SUPPORTING INFORMATION

Additional supporting information may be found in the online version of the article at the publisher's website.

How to cite this article: Qu, Y., Guan, R., Yu, L., Berkowitz, O., David, R., Whelan, J. et al. (2022) Enhanced reactive oxygen detoxification occurs in salt-stressed soybean roots expressing GmSALT3. *Physiologia Plantarum*, 174(3), e13709. Available from: <https://doi.org/10.1111/ppl.13709>